Mass Spectrometry

DOI: 10.1002/anie.200805114

Nanophotonic Ion Production from Silicon Microcolumn Arrays**

*Bennett N. Walker, Trust Razunguzwa, Matthew Powell, Richard Knochenmuss, and Akos Vertes**

Highly confined electromagnetic fields play an important role in the interaction of laser radiation with nanostructures.[1] Near-field optics show great potential in manipulating light on a sub-micrometer scale or even on the molecular scale.[2] Nanophotonics takes advantage of structures that exhibit features commensurate with the wavelength of the radiation. Among other applications, it has been utilized for nanoparticle detection,[3] for the patterning of biomolecules,[4] and for creating materials with unique optical properties.[5] The latter include laser-induced silicon microcolumn arrays (LISMAs), which are produced by ultrafast laser processing of silicon surfaces[6] and are known to have uniformly high absorptance in the 0.2–2.4 μm wavelength range[7] as well as superhydrophobic properties.[8] At sufficiently high laser intensities, the molecules adsorbed on these nanostructures undergo desorption and ionization and eventually exhibit unimolecular decomposition. The resulting ion fragmentation patterns can be used for structure elucidation in mass spectrometry.[9] Manipulation of ion production from biomolecules with photonic structures (i.e., photonic ion sources) based on the interaction of laser light and nanostructures, however, has not previously been demonstrated.

Herein we report a dramatic disparity in the efficiency of ion production from LISMAs depending on the polarization of the incident laser beam. When the electric field of the radiation has a component that is parallel to the column axes (p-polarized beam), the desorption and ionization processes are efficient, whereas if they are perpendicular (s-polarized waves), minimal ion production is observed. These results are also corroborated by studying the ion yield as a function of the incidence angle of an unpolarized laser beam. This strong directionality in ion production is a unique feature of these nanostructures.

LISMAs were created by exposing low-resistivity p-type silicon wafers to 600 pulses from a mode-locked frequency-tripled Nd:YAG laser ($0.13\ J\,cm^{-2}$) in an aqueous environment. The resulting processed areas (ca. 1 mm^2) were covered with quasi-periodic columnar structures that were, on the average, aligned perpendicular to the silicon wafer. Figure 1a,b shows a top view using atomic force microscopy (AFM) and a cross-sectional view using scanning electron microscopy (SEM). The average periodicities of the resulting arrays were determined by taking the 2D fast Fourier transform (FFT) of the SEM image (Figure 1c). A weak ring indicates some nondirectional local periodicity, with a typical spacing of about 500 nm. The schematic depiction in Figure 1d shows the relationship between the laser beam and the microcolumn with the electric field vector for a p-polarized ray $\mathbf{E_i}$, its components parallel ($E_\parallel = E_i \cos\vartheta_i$) and perpendicular ($E_\perp = E_i \sin\vartheta_i$) to the substrate, and the angle of incidence ϑ_i.

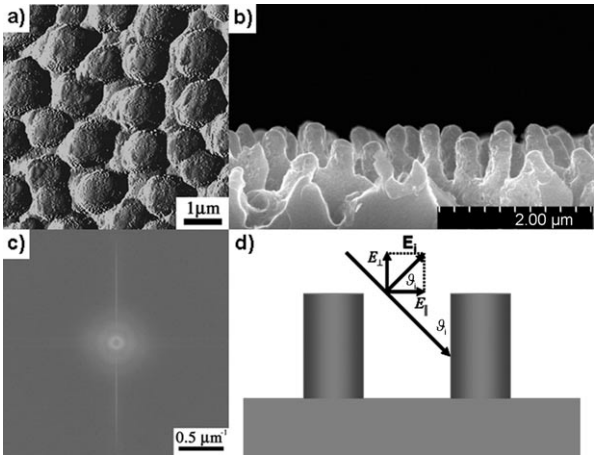

Figure 1. a) Top view by AFM reveals the quasi-periodic arrangement of the microcolumns in LISMA. b) Cross-sectional view by SEM shows an average column height and diameter of approximately 600 and 300 nm, respectively, with 200 nm troughs between the columns. c) Two-dimensional FFT of a top-view image by SEM reveals the approximately 500 nm mean periodicity of LISMA structures. d) Schematic depiction of the incident laser beam microcolumn interaction.

After cleaning and drying, these structures were used as substrates for laser desorption ionization experiments. Experiments were conducted to investigate the ion yields for various organic and biomolecules as a function of substrate orientation with respect to the beam direction for unpolarized laser beams and their dependence on the angle between the plane of incidence and the electric field vector

[*] B. N. Walker, Prof. A. Vertes
The George Washington University, Department of Chemistry
Washington, DC 20052 (USA)
Fax: (+1) 202-994-5873
E-mail: vertes@gwu.edu
Homepage: http://www.gwu.edu/~vertes
Dr. R. Knochenmuss
Novartis Institutes for Biomedical Research
4056 Basel (Switzerland)
Dr. T. Razunguzwa, Dr. M. Powell
Protea Biosciences, Inc.
Morgantown, WV 26507 (USA)

[**] Financial support by the Chemical Sciences, Geosciences and Biosciences Division within the Office of Basic Energy Sciences of the U.S. Department of Energy (DE-FG02-01ER15129) and from the George Washington University Research Enhancement Fund (GWU-REF) is acknowledged.

Supporting information for this article is available on the WWW under http://dx.doi.org/10.1002/anie.200805114.

for polarized laser beams. Typically, 1 μL of sample solution (ca. 0.001mM in 40% methanol) was directly deposited on the LISMA and inserted into a time-of-flight (TOF) mass spectrometer (MS). Similar to matrix-assisted laser desorption ionization (MALDI), pulses from a nitrogen laser were used to produce the ions.

For MALDI, the incidence angle of the desorption laser beam with respect to the sample had no effect on the analyte ion yield[10] and only moderate influence on the total desorption[11] yields. For the polycrystalline samples produced by the common dried droplet sample preparation technique in MALDI, this observation was rationalized in terms of the random orientation of the matrix crystals. On LISMA substrates, however, the average column orientation is perpendicular to the wafer. Moreover, the mean periodicity of the LISMA structure is commensurate with the wavelength of the laser light. Thus, directionality of the interaction between the laser beam and the LISMA structure was explored by altering the sample orientation in the mass spectrometer. The LISMA substrates were mounted on three different facets of a cylindrical sample probe machined to produce 45, 15, and 0° incidence angles. Ion yields for verapamil (see Figure 2a) and the neuropeptide substance P (see Figure S1a in the Supporting Information) revealed a dramatic decrease in ion yield between 45 and 15° and close to zero signal at 0°. From the perspective of a simple illumination geometry argument, these results are counterintuitive, because at 0° incidence angle the troughs between the columns are more exposed to the laser irradiation than in the 45° case.

Conventional MALDI experiments were also conducted on the different facets of the probe using 2,5-dihydroxybenzoic acid (DHB) as the matrix. Figure 2b,c compares the MALDI mass spectra for incidence angles 45 and 0°. The essentially unaltered ion yields indicated that the dramatic decline in ion yields on LISMAs could not be explained by the reduced ion collection efficiency in the source at 0°.

Laser surface processing of silicon at elevated fluences (e.g., ca. 0.8 J cm^{-2}) with plane-polarized beams showed that p-polarized beams, with the electric field vector in the plane of incidence, were the most efficient in producing nanostructures.[12] The p-polarized beam seems to be absorbed more strongly by the perturbed silicon surface than its s-polarized counterpart, for which the electric field is perpendicular to the plane of incidence.[13]

To explore the interaction of electromagnetic waves and LISMAs in desorption ionization experiments, a plane-polarized laser beam was used at typical fluences (ca. 0.1 J cm^{-2}) for ion production from adsorbates. By rotating the plane of polarization from p to s while maintaining the energy of the laser pulse at approximately

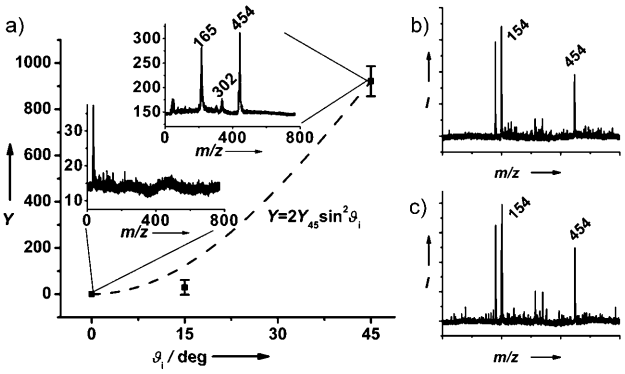

Figure 2. a) Ion yields for verapamil desorbed from a LISMA decrease dramatically between incidence angles of 45 and 15° and vanish at 0°. Insets show the mass spectra for 45 and 0°. MALDI experiments show no change in the spectra for incidence angles of b) 0 and c) 45°. A simple model prediction, analogous to Equation (1), is shown by the dashed curve.

10 μJ, the ion yield from LISMAs showed a dramatic drop. Figure 3 compares the laser desorption ionization spectra for verapamil for unpolarized, p-polarized, and s-polarized beams. Compared to the unpolarized beam in Figure 3a, only a slight decrease in the signal was observed when the LISMA was exposed to the p-polarized ray (Figure 3b), whereas the s-polarized ray (Figure 3c) showed no signal at all. Similar results were obtained for other adsorbates, such as small organic molecules (reserpine) and peptides (leucine enkephalin and substance P), for which a marginal signal or no signal was observed for the s-polarized beam (see Figure S2 in the Supporting Information).

In commonly used soft ionization methods, such as MALDI, polarization dependence of ion yields are not reported. As a control experiment, we studied the MALDI ion yields of verapamil from DHB matrix with plane-polarized laser beams. Figure 4 shows that no significant difference exists between the MALDI spectra using p-polarized and s-polarized rays (Figure 4b,c). This finding can be rationalized by considering the random orientation of the matrix crystals (Figure 4a) in the polycrystalline sample.

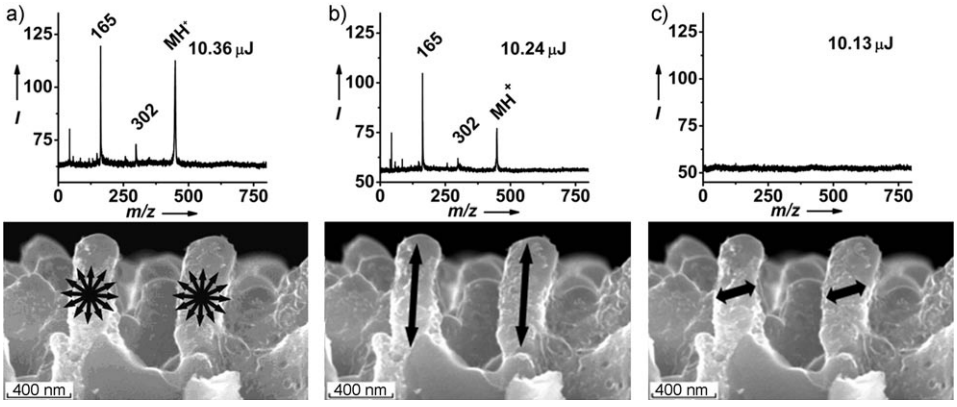

Figure 3. Ion yields from LISMA were compared for laser desorption ionization experiments with a) unpolarized, b) p-polarized, and c) s-polarized rays at approximately 10 μJ per pulse from a nitrogen laser. The p-polarized ray had similar ionization efficiency to the unpolarized ray, whereas no signal was detected with the s-polarized ray.

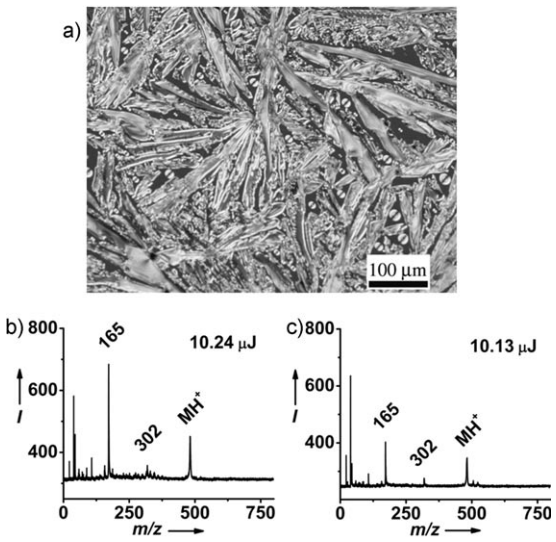

Figure 4. a) Random orientation of matrix crystals is observed in the microscope image of the sample. MALDI mass spectra show no significant change between b) the p-polarized and c) the s-polarized rays.

To investigate the transition in ion production between the s- and p-polarized beams, the total ion yield Y for leucine enkephalin was recorded as a function of polarization angle ϕ_i while a pulse energy of approximately 10 μJ was maintained (Figure 5). As a comparison, the MALDI ion yield from DHB matrix was also recorded. For the LISMA platform, ion production gradually diminished as the plane of polarization was rotated from parallel (p-polarized) to normal (s-polarized) to the plane of incidence, whereas no significant trend was observed for MALDI. Specifically, the LISMA ion yield for the p-polarized ray (Y_p) was approximately 110 times greater than that of the s-polarized ray (Y_s). When we performed these experiments going from the s- to the p-polarized beam, no hysteresis was observed in the ion-yield curve. Similar results were obtained for small organic molecules and peptides, including reserpine, verapamil, and substance P.

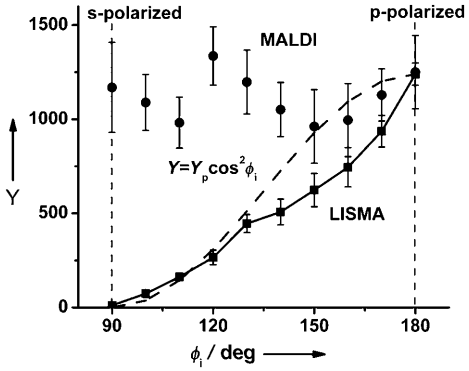

Figure 5. Total ion yields for leucine enkephalin were compared for LISMA (■, ——) and MALDI from DHB matrix (●) as the plane of polarization was rotated from s-polarized to p-polarized while the pulse energies were maintained at approximately 10 μJ. Simple model prediction, analogous to Equation (1), is shown by the dashed curve.

The formation of LISMAs and other laser-induced periodic surface structures (LIPSS; e.g., gratings) demonstrate the resonant interactions of these modulated surfaces with laser radiation of commensurate wavelengths. At elevated fluences, for example 0.4–0.8 J cm^{-2} for 248 nm light impinging on silicon, the formation of these structures is promoted by the interference between the incident and the reflected, refracted, or surface electromagnetic waves (SEW).[14] While below the melting temperature surface acoustic waves (SAW) are formed, laser-modulated capillary waves (CW) dominate with the appearance of a transient molten layer at elevated fluences, and interference evaporation instabilities (IEI) become important with the onset of rapid evaporation.[15]

Similar to the evidence found for the formation of LIPSS, our observations on adsorbate ion yields at low fluences indicate a strong dependence on the angle of incidence (see Figure 2) and on the polarization of the laser light (see Figure 5). Let us examine first if energy deposition by the SEW can explain our observations. The amplitude of SEW is proportional to the projection of the incident wave electric field vector $\mathbf{E}_i$ on the substrate. If the desorption process were to be stimulated by the SEW that is resonant with the LISMA structure, the observed angle dependence of the ion yield could be explained by the variation of the SEW intensity with the incidence angle. For a p-polarized beam with angle of incidence ϑ_i, the substrate projection of the electric field vector is $E_\parallel = E_i \cos\vartheta_i$, predicting maximum SEW intensities for $\vartheta_i = 0°$ with continuous decline as ϑ_i approaches 90°.[14,15] Thus, energy deposition from SEW must not be the driving force behind laser desorption from LISMAs, because the observed ion yields exhibited the opposite trend, that is, they were zero at $\vartheta_i = 0°$ and significantly increased as ϑ_i approached 45°.

For p-polarized incident laser beams, efficient LIPSS[14] and LISMA formation[16] was observed, whereas s-polarized radiation showed no or reduced surface structuring. Analogously, ion yields from adsorbates on LISMAs dramatically decreased when the incident beam polarization was changed from p to s.

A possible explanation of this difference can be based on the difference in laser–surface coupling for axial versus transverse excitation of the columns. The height of the columns is approximately two times the 337 nm wavelength of the desorption laser. This structure and its electrostatic image in the "ground plane" of the bulk substrate would add to form an efficient antenna for p-polarized, but not s-polarized, light. The lateral dimension of the columns is about one wavelength, but the image in the bulk would negate, rather than enhance, the laser-induced polarization. Furthermore, the lateral spacing of 500 nm is about 1.5 wavelengths, so the phase differences between columns lead to cancellation of induced polarization. It seems likely, therefore, that p-polarized laser light is significantly more efficiently absorbed by the columns than s-polarized light. This discrepancy will result in large temperature differences during the laser pulse, which translate into differences in desorption efficiency and ion yield.

In a simple picture, the absorption efficiency depends on the projection of the electric field from a light wave polarized in the ϕ_i plane onto the microcolumns protruding perpendicular to the substrate, $E_\perp = E_i \sin\vartheta_i \cos\phi_i$. Thus the part of the laser intensity that is axially absorbed in the columns can be expressed as in Equation (1), where the incident light

$$I_\perp = I_i \sin^2\vartheta_i \cos^2\phi_i, \quad (1)$$

intensity is $I_i = c\,\varepsilon_0 E_i^2/2$ and ε_0 is the dielectric permittivity in vacuum. The extrema of Equation (1) are consistent with our experimental observations. For right-angle illumination ($\vartheta_i = 0°$) with light of any polarization, there is no axial absorption, because $I_\perp(\vartheta_i{=}0°) = 0$. For a nonzero angle of incidence (e.g., $\vartheta_i = 45°$) p-polarized beams with $\phi_i = 180°$ result in maximum energy deposition, whereas for s-polarized radiation with $\phi_i = 90°$, no axial modes are excited.

Thus, energy deposition by axial absorption in the microcolumns is consistent with our low-fluence ion yield data. The dashed line in Figure 5, $Y = Y_p \cos^2\phi_i$, reflects the polarization angle dependence in Equation (1). For $90° \le \phi_i \le 130°$ and for 180°, the agreement with experimental data is excellent, whereas between 140 and 170° there is a considerable gap between the prediction by this simple model and the measured values. It is likely that in this polarization angle range, additional factors not incorporated into the present model play a significant role. Importantly, above a threshold intensity the linear I_i dependence in Equation (1) prevails when the angle of incidence and the polarization are kept constant (see Figure S3 in the Supporting Information).

Further testing of our hypothesis based on the role of axial absorption modes in laser desorption from LISMAs can be carried out by changing the aspect ratio h/d and the height-to-wavelength ratio h/λ of the microcolumns. If this hypothesis is correct, as the aspect ratio approaches $h/d < 1$ the influence of the angle of incidence and the polarization angle on the ion yield is expected to diminish. Similarly, the length of the columns in wavelength units (h/λ) will affect the efficiency of coupling of the laser energy to the LISMA structure.

In the laser desorption of adsorbates, the aspect ratio of troughs (h/t, where t is the width of the troughs) impacts a different set of processes. The ability to retain residual solvent molecules and large amounts of adsorbate increases with h/t. Nanoporous desorption substrates in desorption ionization on silicon (DIOS)[17] and in nanostructure-initiator mass spectrometry (NIMS)[18] are extreme examples of structures with high trough aspect ratios. As the laser pulse produces a plume from these species, owing to confinement effects, the plume density, persistence, and chemistry are enhanced for high trough aspect ratios.[19]

The ion production properties on LISMAs described herein represent the first example of nanophotonically modulated ion sources. Owing to their structure, energy coupling between the LISMAs and the laser radiation is fundamentally different from MALDI, DIOS, and NIMS. Thus, they enable the control of ion production by varying laser radiation properties other than simple pulse energy, in particular the angle of incidence and the plane of polarization. Photonic ion sources promise to enable enhanced control of ion production on a micro- and nanometer scale and direct integration with microfluidic devices.

Experimental Section

Low-resistivity, p-type mechanical grade silicon chips (surface area ca. 3 mm^2) were placed in a water processing environment and exposed to repeated laser irradiation from a mode-locked frequency-tripled Nd:YAG laser with 355 nm wavelength and 22 ps pulse length, producing a 1 mm diameter laser spot. The resulting processed spot with the LISMAs was placed in a time-of-flight mass spectrometer (TOF-MS) for soft laser desorption ionization experiments using unpolarized and polarized nitrogen laser beams. Polarization was achieved using a Glan–Taylor calcite polarizer, and the polarized beam was attenuated with a neutral density filter to maintain a consistent pulse energy of approximately 10 μJ. Experiments were conducted on a home-built TOF-MS.[20] Additional details on the materials and methods are provided in the Supporting Information.

Received: October 18, 2008
Published online: January 23, 2009

Keywords: laser desorption ionization · laser spectroscopy · mass spectrometry · nanophotonics · nanostructures

[1] C. Girard, *Rep. Prog. Phys.* **2005**, *68*, 1883.
[2] T. H. Taminiau, F. D. Stefani, F. B. Segerink, N. F. Van Hulst, *Nat. Photonics* **2008**, *2*, 234.
[3] B. Schmidt, V. Almeida, C. Manolatou, S. Preble, M. Lipson, *Appl. Phys. Lett.* **2004**, *85*, 4854.
[4] P. Bhatnagar, S. S. Mark, I. Kim, H. Y. Chen, B. Schmidt, M. Lipson, C. A. Batt, *Adv. Mater.* **2006**, *18*, 315.
[5] S. Coyle, M. C. Netti, J. J. Baumberg, M. A. Ghanem, P. R. Birkin, P. N. Bartlett, D. M. Whittaker, *Phys. Rev. Lett.* **2001**, *87*, 17.
[6] T. H. Her, R. J. Finlay, C. Wu, S. Deliwala, E. Mazur, *Appl. Phys. Lett.* **1998**, *73*, 1673.
[7] C. H. Crouch, J. E. Carey, J. M. Warrender, M. J. Aziz, E. Mazur, F. Y. Genin, *Appl. Phys. Lett.* **2004**, *84*, 1850.
[8] V. Zorba, L. Persano, D. Pisignano, A. Athanassiou, E. Stratakis, R. Cingolani, P. Tzanetakis, C. Fotakis, *Nanotechnology* **2006**, *17*, 3234.
[9] Y. Chen, A. Vertes, *Anal. Chem.* **2006**, *78*, 5835.
[10] A. Westman, T. Huthfehre, P. Demirev, J. Bielawski, N. Medina, B. U. R. Sundqvist, *Rapid Commun. Mass Spectrom.* **1994**, *8*, 388.
[11] A. P. Quist, T. Huthfehre, B. U. R. Sundqvist, *Rapid Commun. Mass Spectrom.* **1994**, *8*, 149.
[12] A. J. Pedraza, J. D. Fowlkes, Y. F. Guan, *Appl. Phys. A* **2003**, *77*, 277.
[13] T. H. Her, R. J. Finlay, C. Wu, E. Mazur, *Appl. Phys. A* **2000**, *70*, 383.
[14] A. J. Pedraza, Y. F. Guan, J. D. Fowlkes, D. A. Smith, *J. Vac. Sci. Technol. B* **2004**, *22*, 2823.
[15] S. A. Akhmanov, V. I. Emelyanov, N. I. Koroteyev, V. N. Seminogov, *Uspekhi Fizicheskikh Nauk* **1985**, *147*, 675.
[16] J. E. Carey, Ph.D. dissertation (Harvard University) **2004**.
[17] J. Wei, J. M. Buriak, G. Siuzdak, *Nature* **1999**, *399*, 243.
[18] T. R. Northen, O. Yanes, M. T. Northen, D. Marrinucci, W. Uritboonthai, J. Apon, S. L. Golledge, A. Nordstrom, G. Siuzdak, *Nature* **2007**, *449*, 1033.
[19] G. H. Luo, Y. Chen, G. Siuzdak, A. Vertes, *J. Phys. Chem. B* **2005**, *109*, 24450.
[20] Y. Chen, A. Vertes, *J. Phys. Chem. A* **2003**, *107*, 9754.

